

SUPPLEMENTARY INFORMATION

In depth transcriptomic profiling defines a landscape of dysfunctional immune responses in patients with VEXAS syndrome

Hiroki Mizumaki,^{1,*} Shouguo Gao,^{1,*} Zhijie Wu,¹ Fernanda Gutierrez-Rodrigues,¹ Massimiliano Bissa,² Xingmin Feng,¹ Emma M. Groarke,¹ Haoran Li,¹ Lemlem Alemu,¹ Diego Quinones Raffo,¹ Ivana Darden,¹ Sachiko Kajigaya,¹ Peter C. Grayson,³ Genoveffa Franchini,² Neal S. Young,^{1,†} and Bhavisha A. Patel,^{1,†}

* These authors contributed equally.

† These authors jointly supervised this work.

¹ Hematology Branch, National Heart, Lung, and Blood Institute, National Institutes of Health, Bethesda, MD, United States

² Animal Models and Retroviral Vaccines Section, National Cancer Institute, National Institutes of Health, Bethesda, MD, United States

³ Vasculitis Translational Research Program, National Institute of Arthritis and Musculoskeletal, and Skin Diseases, National Institutes of Health, Bethesda, MD, United States

Supplementary Tables

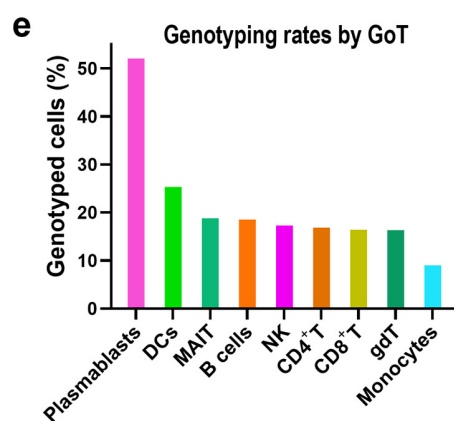
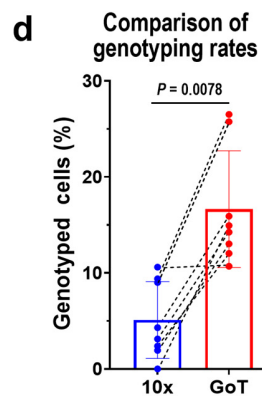
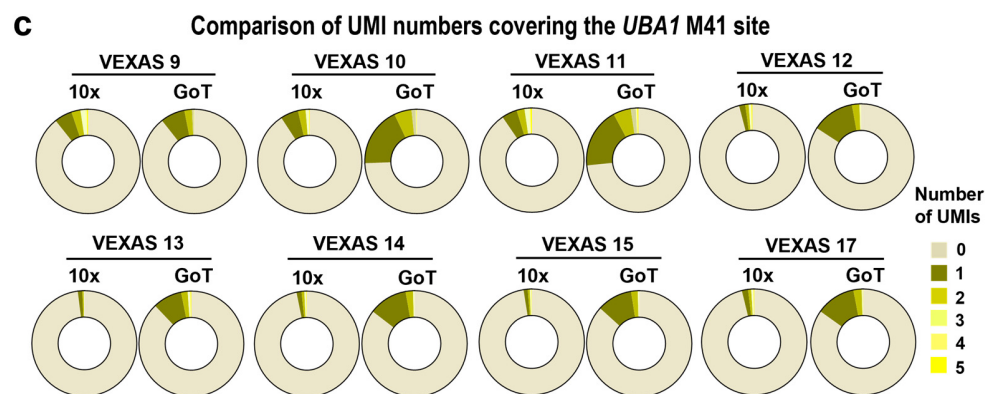
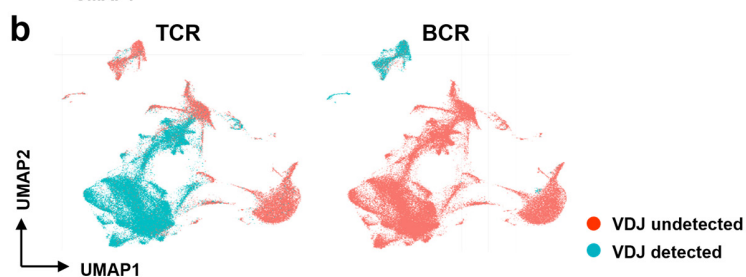
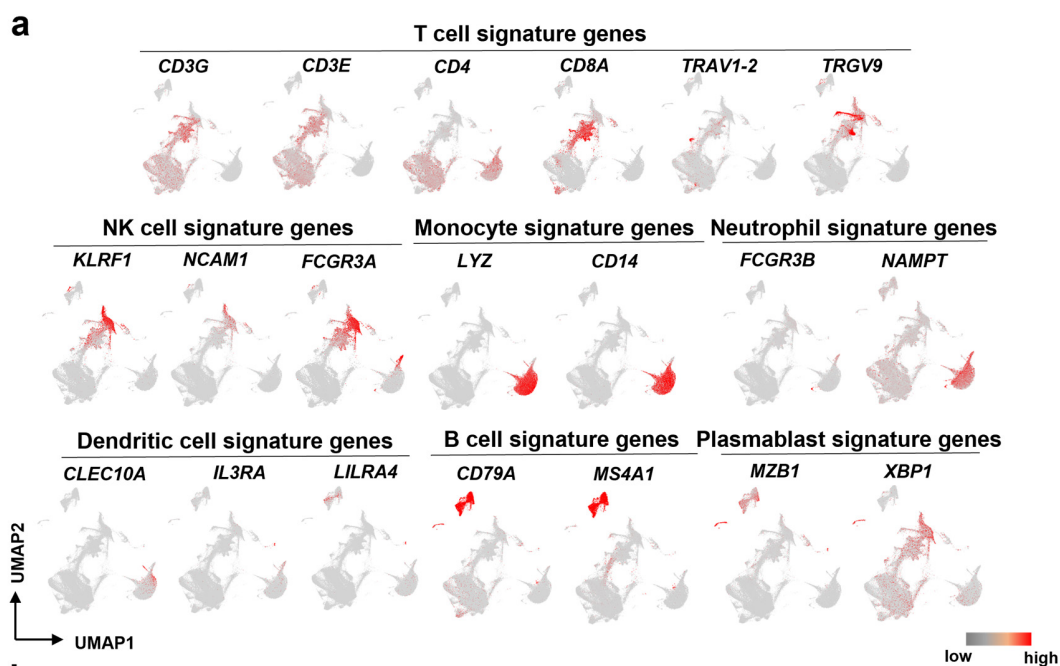
Supplementary Table 1. Clinical and laboratory characteristics of patients with VEXAS syndrome

Supplementary Table 2. *UBA1* genotyping metrics in 10x gene expression data and GoT libraries

Supplementary Table 3. Differentially expressed genes in monocytes from VEXAS

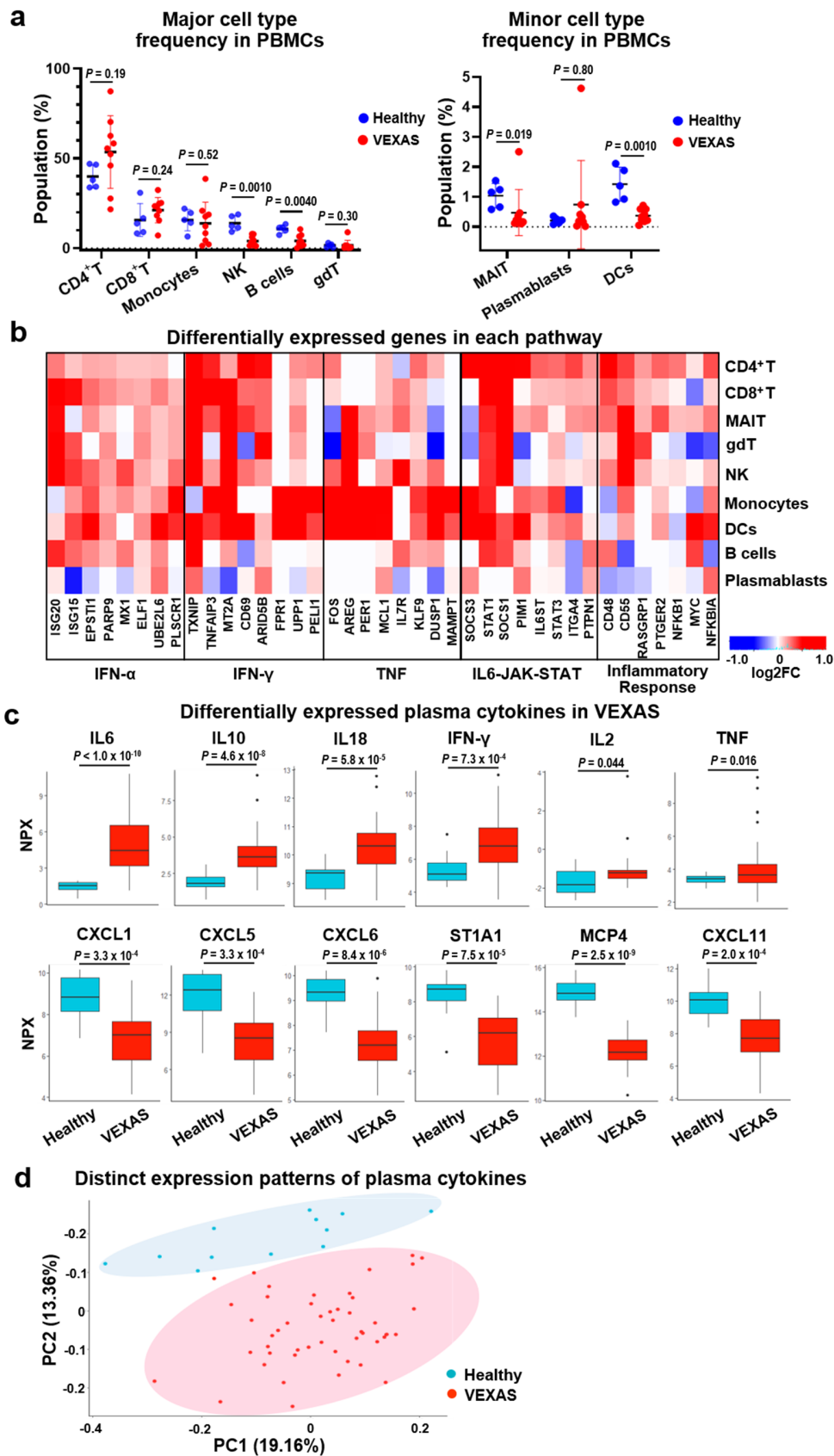
Supplementary Table 4. Differentially expressed genes in *UBA1*-mutated NK cells

Supplementary Table 5. Sequences of TCR groups with more than five different clones obtained from GLIPH2 analysis

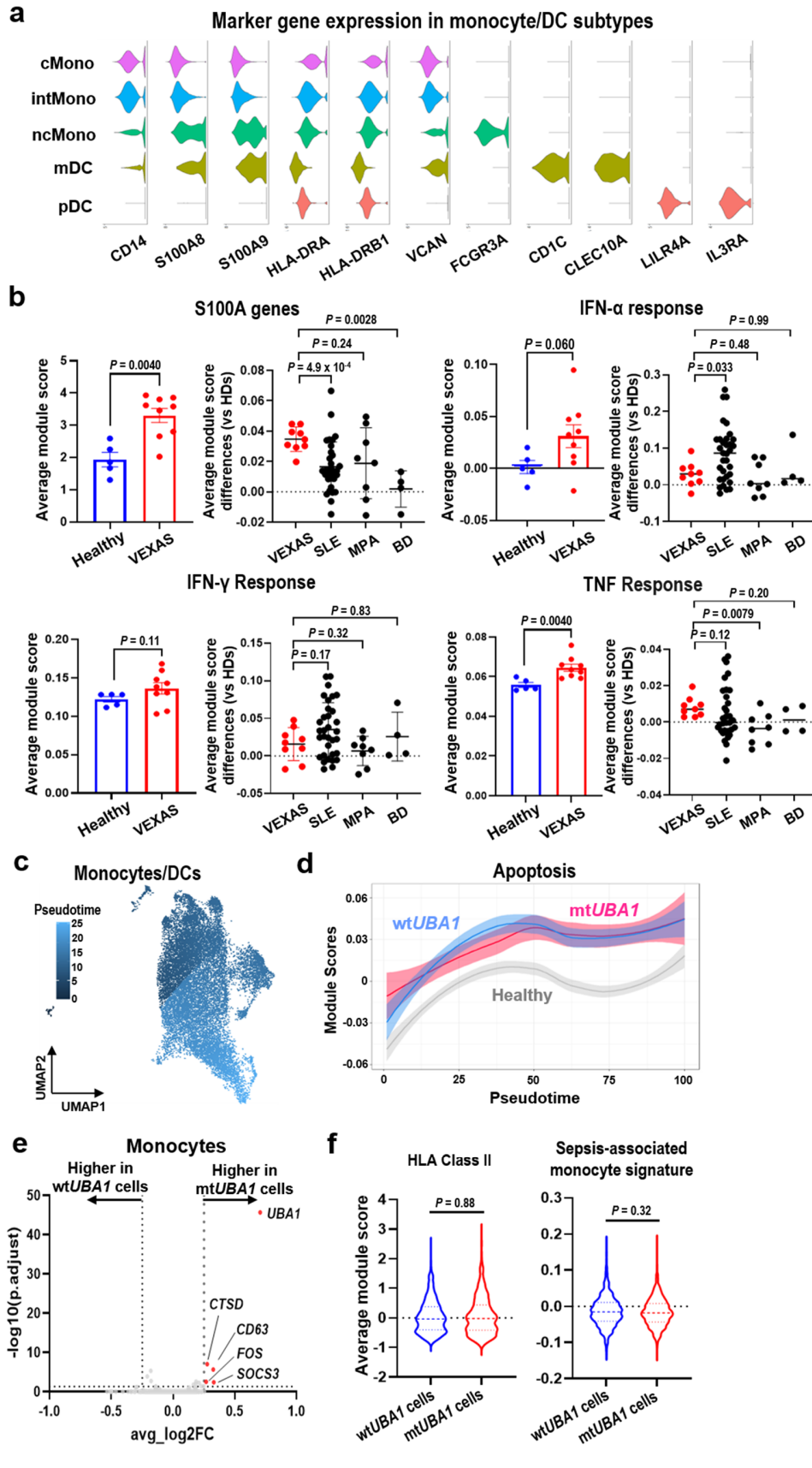


Supplementary Fig. 1: Cell type annotation and genotyping of PBMCs from VEXAS patients.

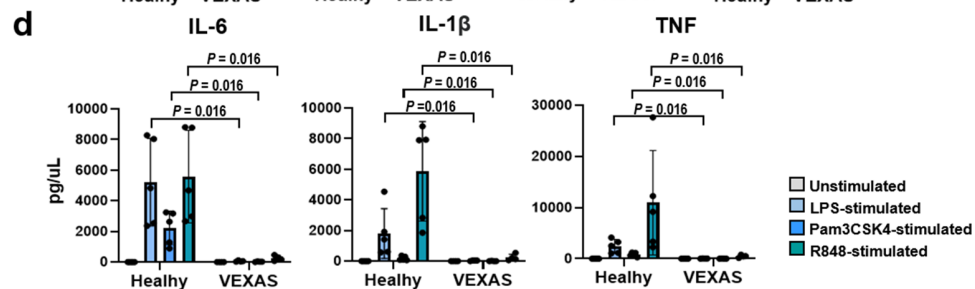
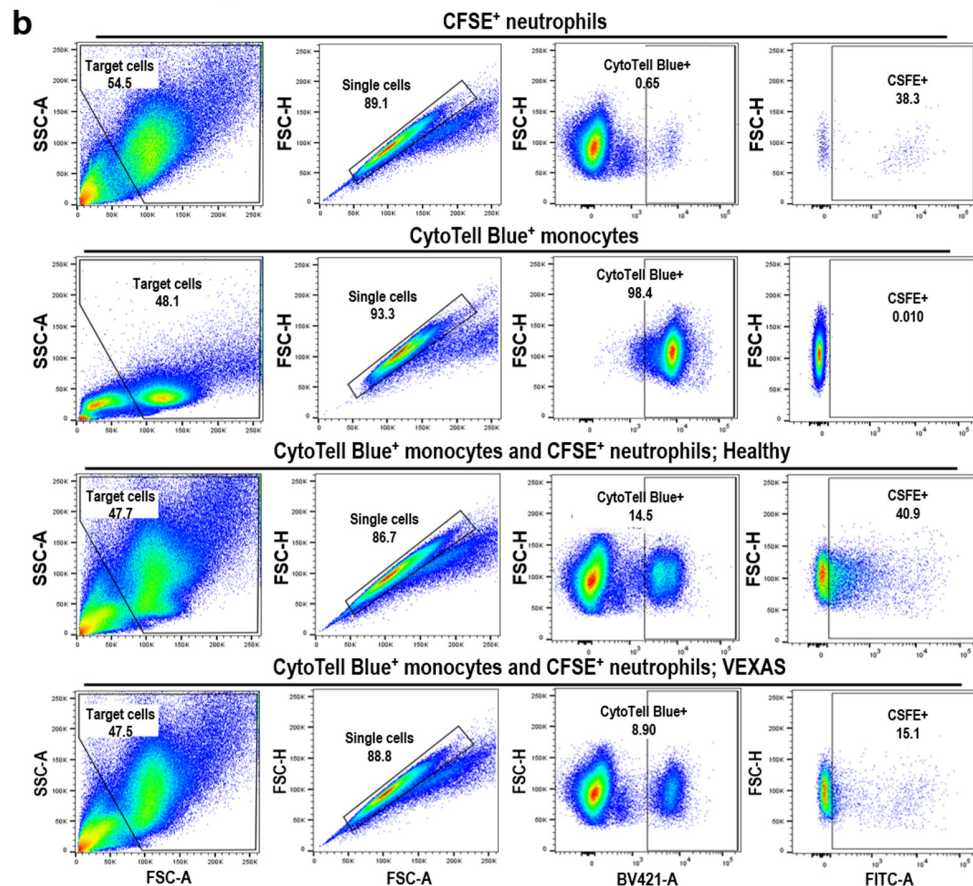
a, Expression of cell-type specific genes highlighted in uniform manifold approximation and projection (UMAP) plots of peripheral blood mononuclear cells (PBMC) from all VEXAS patients and healthy donors. **b**, Expression of TCR (left) and BCR (right) highlighted in UMAP plots of PBMCs of all VEXAS patients and healthy donors. **c**, Fractions of cells by the numbers of unique molecular identifier (UMI) with the *UBA1 M41* locus coverages in standard 10x gene expression data processed with *cb_sniffer* (left) and UMIs with *UBA1 M41* locus coverages in genotyping of transcriptomes (GoT) amplicon libraries (right) (see Supplementary Table 2 for cell numbers in each sample). **d**, Comparison of genotyping rates obtained from standard 10x gene expression data (n = 8) and GoT data (n = 8). Data are presented as a mean value with SD. *P* values were calculated using the two-sided Wilcoxon matched-pairs signed rank test. **e** Genotyping rates through GoT in major cell types. Cell types with more than 100 cells were analyzed. DCs, dendritic cells; MAIT, mucosa-associated invariant T cell; gdT, gamma delta T cells.



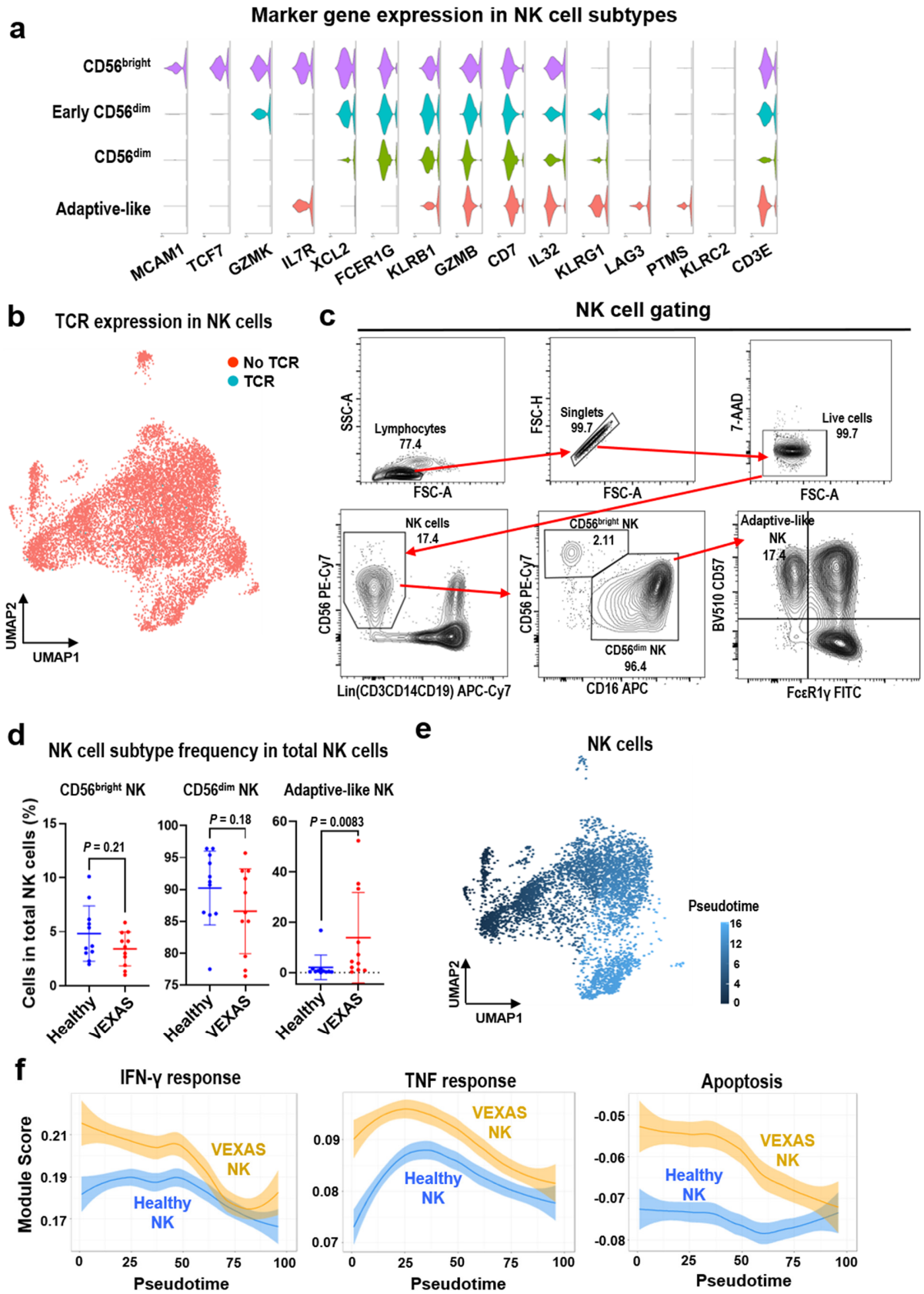
Supplementary Fig. 2: Differences in cellular composition, gene expression, and cytokine production between VEXAS patients and healthy donors. **a**, Percentages of each major cell type relative to the total number of PBMCs derived from VEXAS patients (n = 9, red dots) and healthy donors (n = 5, blue dots): major cell types with an average ratio of 2% or greater (left), and less than 2% (right). Data are presented as a mean value with SD. *P* values were calculated using the two-sided unpaired Mann-Whitney *U* test. **b**, Heatmap showing expression of differentially expressed representative genes grouped by their functional pathways in IFN- α signaling, IFN- γ signaling, TNF signaling, IL6-JAK-STAT signaling, and inflammatory response pathways among the major cell types of VEXAS patients (n = 9) as compared to those of healthy donors (n = 5). Values are presented as log2-fold change (FC). **c**, Box and whisker plots showing normalized plasma protein expression (NPX) levels of IL-6, IL-10, IL-18, IFN- γ , IL-2, TNF, CXCL1, CXCL5, CXCL6, ST1A1, MCP4, and CXCL11. A box plot shows median and interquartile ranges (IQR); Lower and upper hinges correspond to the first and third quartiles. A upper whisker extends from the hinge to the largest value no further than 1.5*IQR from a hinge. A lower whisker extends from the hinge to the smallest value at most 1.5*IQR from the hinge. *P* values were calculated using the two-sided unpaired Mann-Whitney *U* test. **d**, Principal component (PC) analysis plot of individual plasma samples based on cytokine expression levels measured by the Olink inflammatory panel multiplex immunoassay. Each dot represents one individual sample from VEXAS patients (red dots) and from healthy donors (blue dots). DCs, dendritic cells; MAIT, mucosa-associated invariant T cells; gdT, gamma delta T cells.



Supplementary Fig. 3: Immunological features of monocytes in VEXAS. **a**, Violin plot showing expression distributions of selected canonical markers in five subtypes of monocytes and dendritic cells (DC). Rows and columns represent selected marker genes and cell types, respectively. **b**, Gene module scores of alarmin-related S100A genes, IFN- α response, IFN- γ response, and TNF response pathways in monocytes across VEXAS ($n = 9$), healthy donors ($n = 5$), and other multisystem autoimmune diseases (Systemic lupus erythematosus (SLE), $n = 33$; microscopic polyangiitis (MPA), $n = 8$; Behcet's disease (BD), $n = 4$). For comparison among diseases, differences of gene module scores between VEXAS and healthy donors are displayed. Data are presented as mean with SD. P values were calculated using two-sided unpaired Mann-Whitney U test. **c**, UMAP plot visualizing pseudotime trajectories of all monocytes/DCs in VEXAS. A color code indicates cellular moments in the calculated pseudotime. **d**, Dynamic changes of gene module scores of the apoptosis pathway in wild-type *UBAI* (wt*UBAI*) and *UBAI*-mutated (mt*UBAI*) monocytes from VEXAS and monocytes from healthy donors along differentiation. Data are presented as a mean value with $1.96 \times \text{SE}$. x axis, pseudotime ordering from classical monocytes to nonclassical monocytes estimated by slingshot; y axis, gene module scores of apoptosis pathway. **e**, Volcano plots of differentially expressed genes between wt*UBAI* and mt*UBAI* monocytes. A horizontal dotted line and vertical dotted lines represent an adjusted p value ($p_{\text{adj}} = 0.05$) and absolute $\log_2\text{FC} = 0.25$, respectively. Genes upregulated in mt*UBAI* monocytes (red) are highlighted. P values were calculated with a two-sided Wilcoxon rank-sum test and Bonferroni correction for multiple comparisons. **f**, Gene module scores in wt*UBAI* and mt*UBAI* monocytes for HLA class II genes and sepsis-associated monocyte signature scores. P values were calculated using the two-sided unpaired Mann-Whitney U test.

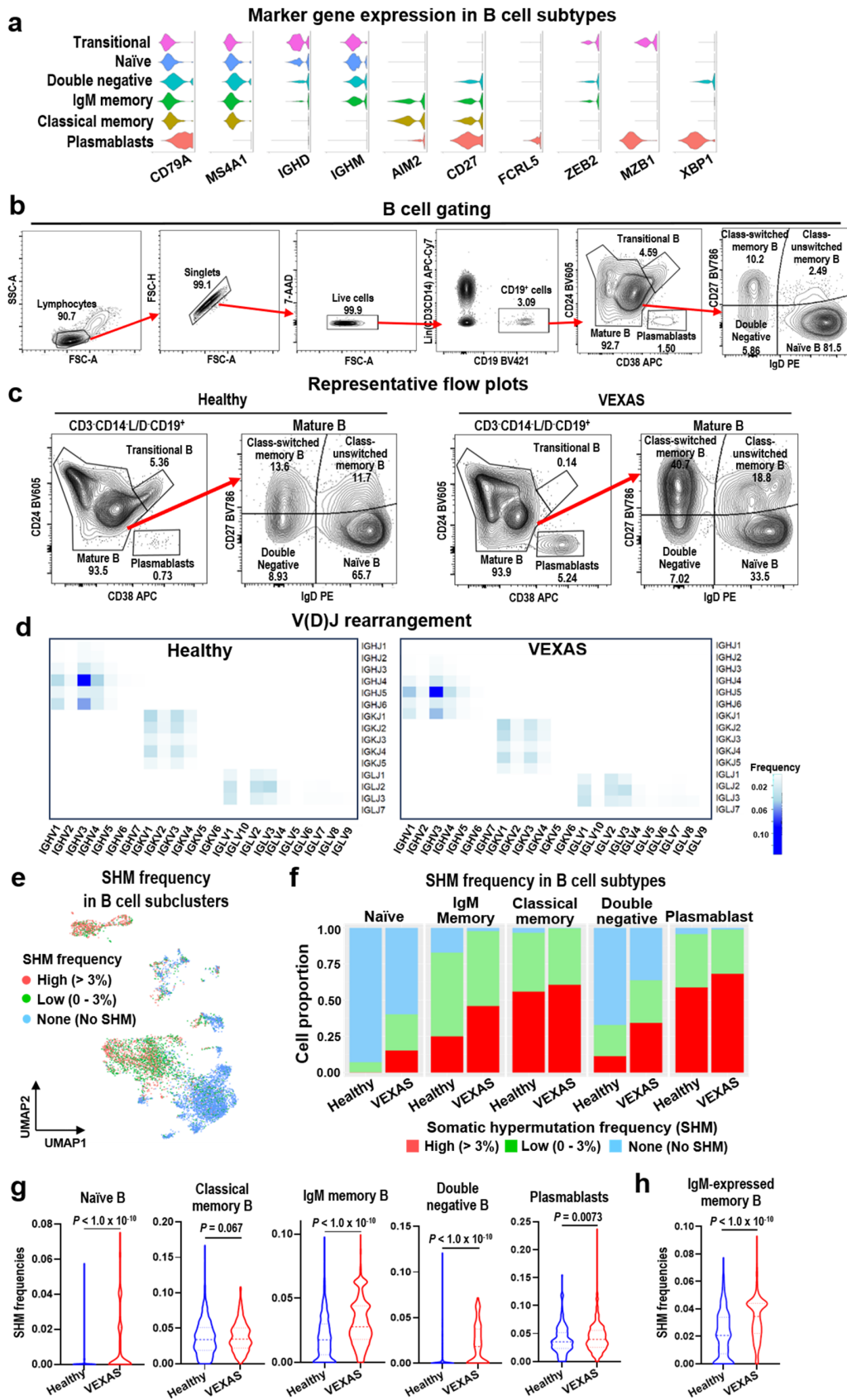


Supplementary Fig. 4: Functional in vitro assay using CD14⁺ monocytes from VEXAS patients. **a**, Schematic representation of the efferocytosis assay. Neutrophils isolated from fresh blood of an unrelated healthy donor were stained with CFSE and induced apoptosis with Staurosporine. CD14⁺ monocytes isolated from frozen peripheral blood mononuclear cells (PBMC) of VEXAS patients and healthy donors were stained with CytoTell Blue. CFSE-labeled apoptotic “bait” neutrophils were then cocultured with “effector” CD14⁺ monocytes overnight. Frequency of CFSE⁺ apoptotic cell uptake in CytoTell Blue⁺ efferocytes (CD14⁺ monocytes) were measured with a flow cytometer. Figure was created in BioRender. Mizumaki, H. (2025) [<https://BioRender.com/w79k163>]. **b**, Representative flow plots showing a gating strategy for identifying efferocytes that engulfed apoptotic neutrophils. Cells were gated on monocytes/neutrophils, singlets, CytoTell Blue⁺ and CFSE⁺. Frequency of efferocytes was expressed as frequency of CFSE⁺ cells in CytoTell Blue⁺ monocytes. CFSE⁺ neutrophils (upper panel) and CytoTell Blue⁺ monocytes (second panel) not cocultured were used as controls for setting the gates. Representative third and bottom panels show cocultured CFSE⁺ neutrophils and CytoTell Blue⁺ monocytes from a healthy donor and a VEXAS patient, respectively. **c**, Cytokine detection of IL-18, IL-10, TNF, and IL-8 in culture supernatants of purified CD14⁺ monocytes (VEXAS patients, n = 10; healthy donors, n = 10) after 8 h in-vitro incubation with or without 100 ng/mL of lipopolysaccharide (LPS). Data are presented as a mean value with SD. *P* values were calculated using the two-sided unpaired Mann-Whitney *U* test. **d**, Cytokine detection of IL-6, IL-1β, and TNF in culture supernatants of purified CD14⁺ monocytes (VEXAS patients, n = 4; healthy donors, n = 5) after 8 h in-vitro incubation with or without 100 ng/mL of lipopolysaccharide (LPS), 100 ng/mL of Pam3CSK4, and 2.5 μM of R848. Data are presented as mean with SD. *P* values were calculated using the two-sided unpaired Mann-Whitney *U* test.



Supplementary Fig. 5: Immunological features of NK cells in VEXAS. **a**, Violin plot of gene expression distributions of selected canonical markers in the four NK cell subtypes. Rows and columns show selected marker genes and represent cell types. **b**, UMAP plot embedding of expression of TCR in subclustered NK cells. **c**, Representative flowcharts for identification of adaptive-like NK cells in peripheral blood. Adaptive-like NK cells were identified as (lowSSC/Singlets/Live/CD56⁺CD3⁻CD14⁻CD19⁻/CD16⁺CD56^{dim}/CD57⁺FcεR1γ). **d**, Proportions of NK cell subtypes relative to the total number of NK cells in healthy donors (n = 11, blue dots) and VEXAS patients (n = 11, red dots) by flow cytometry. Data are presented as a mean value with SD. *P* values were calculated using the two-sided unpaired Mann-Whitney *U* test. **e**, UMAP plot visualizing the pseudotime trajectory of all NK cells in VEXAS. Color code indicates cellular moments in the calculated pseudotime. **f**, Dynamic changes of gene module scores of the IFN-γ response, TNF#response and apoptosis pathways in NK cells from VEXAS patients and healthy donors along differentiation. Data are presented as a mean value with 1.96*SE. x axis, pseudotime ordering from CD56^{bright} NK cells to adaptive-like NK cells estimated by slingshot; y axis, gene module scores for each pathway.

Supplementary Fig. 6: Immunological features of T cells and TCR analysis. **a**, Violin plot showing expression distributions of selected canonical cell markers in ten T cell subtypes. Rows and columns represent clusters and selected marker genes, respectively. **b**, Heatmap showing the numbers of common TCR clones in VEXAS patients ($n = 9$) and healthy donors ($n = 5$) among top 200 TCR clones. Both x- and y-axes indicate samples of VEXAS patients and healthy donors. Numbers indicate counts of identical TCR clones shared among samples. A color scheme ranging from dark orange to blue represents the numbers of shared CDR sequences from high to low. In general, there was few common TCR usage in VEXAS patients or healthy donors. There was also few common TCR usage among VEXAS patients and healthy donors. **c**, Dot plot showing gene set enrichment scores of top 10 upregulated hallmark pathways across $CD8^+$ T cell subtypes. Dot size indicates mean normalized enrichment score (NES) difference between VEXAS patients and healthy donors, and color scale indicates false discovery rate (FDR) value. Non-significant pathways ($FDR \geq 0.10$) are in grey. **d**, UMAP plot illustrating the pseudotime trajectory of all $CD8^+$ T cells. A color code indicates cellular moments in the calculated pseudotime. **e**, Gene module scores in expanded $CD8^+$ T cells from healthy donors versus those of VEXAS patients for IFN- γ response, and T-cell mediated cytotoxicity and exhaustion pathways.



Supplementary Fig. 7: Immunological features of B cells and TCR analysis. **a**, Violin plot of gene expression distributions of selected canonical cell markers in six B cell subtypes. Rows and columns indicate clusters and selected marker genes. **b**, Identification of B cell subsets in peripheral blood. **c**, Representative flow plots for B cell subsets in peripheral blood from VEXAS patients (right) and healthy donors (left). **d**, V(D)J rearrangement differences between VEXAS patients and healthy donors. Colors indicate usage percentages of specific V-J gene pairs. **e**, UMAP plot embedding subclustered B cells colored by levels of somatic hypermutation (SHM) in their corresponding BCRs. Cells with both scRNA-seq data and scBCR-seq data are shown. **f**, SHM frequency distribution in each B-cell subtype according to VEXAS and healthy donors. **g**, Comparison of SHM frequency between each B cell subtype of VEXAS patients and that of healthy donors. *P* values were calculated using the two-sided unpaired Mann-Whitney *U* test. **h**, Comparison of SHM frequency between IgM-expressed memory B cells of VEXAS patients and those of healthy donors. *p* values were calculated using the two-sided unpaired Mann-Whitney *U* test.